Electronic Supplementary Material (ESI) for Reaction Chemistry & Engineering.

Making Photocatalysts Screenable - A Milli Scale Multi-Batch Screening Photoreactor as Extension for the Modular Photoreactor (Supporting Information)

Daniel Kowalczyk[a], Gergely Knorr[b], Kalina Peneva[b*], Dirk Ziegenbalg[a*]

[a]Institute of Chemical Engineering, Ulm University, Albert-Einstein-Allee 11, 89081 Ulm, Germany,

[b]Institute of Organic Chemistry and Macromolecular Chemistry, University of Jena, Lessingstr. 8, 07743 Jena, Germany; Jena Center for Soft Matter, Friedrich Schiller University Jena, Philosophenweg 7, 07743 Jena, Germany; Center for Energy and Environmental Chemistry, Friedrich Schiller University Jena, Philosophenweg 7a, 07743 Jena, Germany

Table of Contents

Materials and Methods

Reagents and Instruments

Reagents and solvents:

Tris(2,2'-bipyridine)ruthenium(II) hexafluorophosphate (97 %), L-ascorbic acid (99 %) were purchased from Sigma Aldrich. Methanol (≥99.8 %) and abs. Ethanol (≥99.5 %) were purchased from VWR International GmbH, aqueous ammonia solution (≥25 %, extra pure) was purchased from Carl Roth GmbH + Co. KG. All solvents and chemicals were purchased in commercial grade (Acros, Alfa Aeser, Deutero, Eurisotop, Fisher, Grüssing, Merck, Roth, Sigma Aldrich, TCI and VWR) and unless otherwise stated, used as obtained. For sample preparation inside the glove box, all solvents were purged with argon for 1 minute per milliliter. The $(NH_4)_2[Mo_3S_{13}]$ x $2H_2O$ catalyst (Mo_3S_{13}-CAT) was synthesized according to an adapted procedure applied by Kowalczyk et. al first described by Müller et. al.[1][2] Water was deionized prior to use. The Bimane compounds 2,3,5,6-tetramethyl-1H,7H-pyrazolo[1,2-a]pyrazole-1,7-dione (syn-Bimane) and 2,6-dibromo-3,7-dimethyl-1H,5H-pyrazolo[1,2-a]pyrazole-1,5-dione (anti-Bimane) were synthesized following the procedure described below. 1,3,3-Trimethylindolino-6'-nitrobenzopyrylospiran (spiropyrane) was purchased from TCI Deutschland GmbH.

Instruments:

Hydrogen evolution was quantified using an Agilent Technologies 7820A GC-TCD by injecting 100 µL of the head space using an Agilent Technologies AOC-20i Plus Autosampler. For sampling a Shimadzu gas tight syringe (250F-S-GT-0.63 250UL SYRINGE) was used. Sample preparation under inert conditions was performed in an MBRAUN LABSTAR glovebox or under Ar flow. For the catalytic experiments, the multi-batch screening photoreactor was equipped with two LED modules assembled of three LEDs each. Depending on the absorption properties of the used photosensitizers, either LST1-01F06-RYL1-00 Deep Blue (λ = 455 nm), LZ4-40B208-0000 (λ = 453 nm) or LST1-01G01-UV01-00 (λ = 365 nm) LED emitters were used.

Experimental Setup

To ensure the protection of eyesight from high intensity visible and UV irradiation during photoreactor operation, the multi-batch screening photoreactor was encased with red Plexiglas with a thickness of 3 mm (see Figure 1 left). The Plexiglas cover was equipped with two 12 V DC fans (manufacturer: Arctic; model number: AFACO-090PC-GBA01) (see Figure 1 left) and operated with a flow rate of 73.1 $m^3 \cdot h^{-1}$. The fans were operated at maximum settings and controlled by the modular controller.[1]

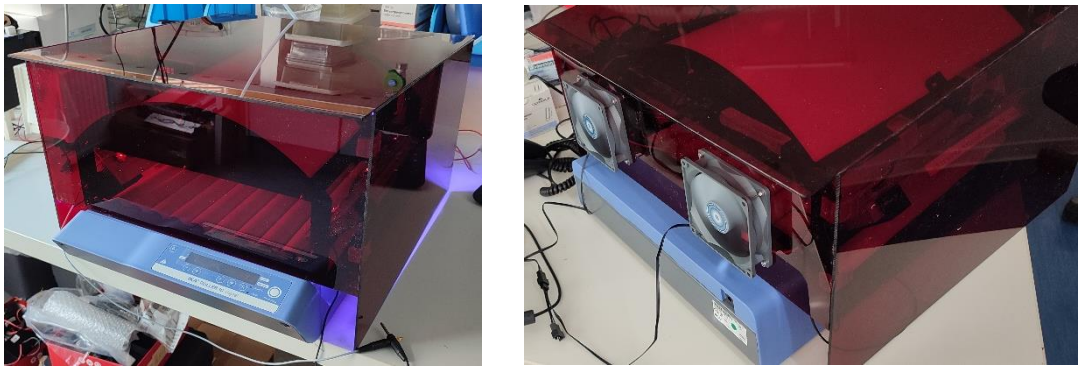

Figure 1: Front and back view of the red Plexiglas cover, with two fans for reactor ventilation on the backside.

Characterized LEDs

Table 1: Characterized LED and product numbers.

LED	Manufacturer	Product Number
365 nm	New Energy	LST1-01G01-UV01-00
455 nm	New Energy	LST1-01F06-RYL1-00
453 nm	LED Engin	LZ4-40B208-0000
530 nm	New Energy	LST1-01F06-GRN1-00

UV/vis Measurement Setup

UV/vis measurement of the spiropyrane/merocyanine mixtures were performed in the measurement setup depicted in Figure 2, consisting of an Avantes AvaLight-DHc deuterium halogen light source, a 3D printed UV/vis measurement cell for cylindrical 4 mL GC vials (see ESI: UV_vis_cell_4mL_GC_vial_SLA.stl), equipped with two COL-UV/VIS collimating lenses fixed with the corresponding UNF 3/8"-24 nuts. The cell was connected to an Avantes AvaSpec-Mini2048CL compact spectrometer connected to a Laptop for measurement data processing. Avantes FC-UVIR600-2 (600 µm) light conducting fiber-optic cables were used to connect the optical components.

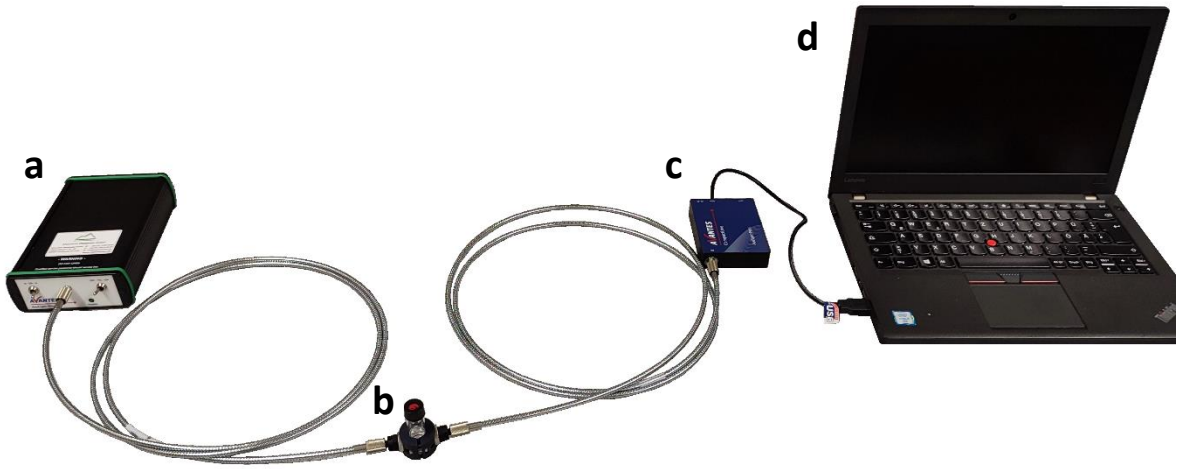

*Figure 2: UV/vis measurement setup consisting of an Avantes AvaLight-DHc deuterium Halogen light source **a,** connected with a Avantes FC-UVIR600-2 (600 µm) fiber-optic cable to a 3D printed UV/vis measurement cell for cylindrical 4 mL GC vials **b**, connected with the same model of fiber-optic cable to an Avantes AvaSpec-Mini2048CL compact spectrometer **c**, and a Laptop for measurement data processing **d.***

Photocatalytic Hydrogen Evolution Catalysis

[Mo_3S_{13}] Catalyzed Hydrogen Evolution

Sample Preparation and Photocatalysis

Following the procedure described for HER catalysis in literature[1] with a 9:1 MeOH/H_2O ratio, stock solutions of ascorbic acid 1 M (AA1), $Ru(bpy)_3(PF_6)_2$ photosensitizer (Ru-PS) and Mo_3S_{13}-CAT where prepared. In addition, a 2 M stock solution of ascorbic acid (AA2) was prepared, the pH was adjusted to 4 using NH_3 (NH_3/H_2O 25 % m/m).

Reproduction of activity in benchmark system and H2 loss over time

2 mL samples of the catalytic system Mo_3S_{13} system described for the evaluation of the modular photoreactor were prepared in 4 mL GC-vials, following the procedure for the 9:1 MeOH/H_2O ratio.[1] Catalysis was performed using a 453 nm LED (*I* = 1 A) without stirring and irradiating the samples for 2 h at room temperature. Two Modular Photoreactors (corpus module 90x90x90 mm, material: white PLA), equipped with 8 vials each in the 8-sample holder of the modular photoreactor fixed at z-position 7 and a fan were used in parallel, resulting in 16 catalytic samples in total.

To rule out hydrogen loss over time, the catalytic samples were stored in the dark and probed in triplicates after 0 h, 0.5 h, 1 h, 2 h and 4 h. One sample was stored for 8 h before probing. As depicted in Figure 3 a significant hydrogen loss could not be observed over time. Over the performed experiments an average TON of 30046 with an maximal standard deviation of around 2.8 % could be determined, which is in good alignment with literature.[1]

Catalytic conditions: [catalyst] = 0.3 µM; [photosensitizer] = 20 µM; [Ascorbic Acid] = 100 mM; Solvent = MeOH/H_2O 90:10 % v:v

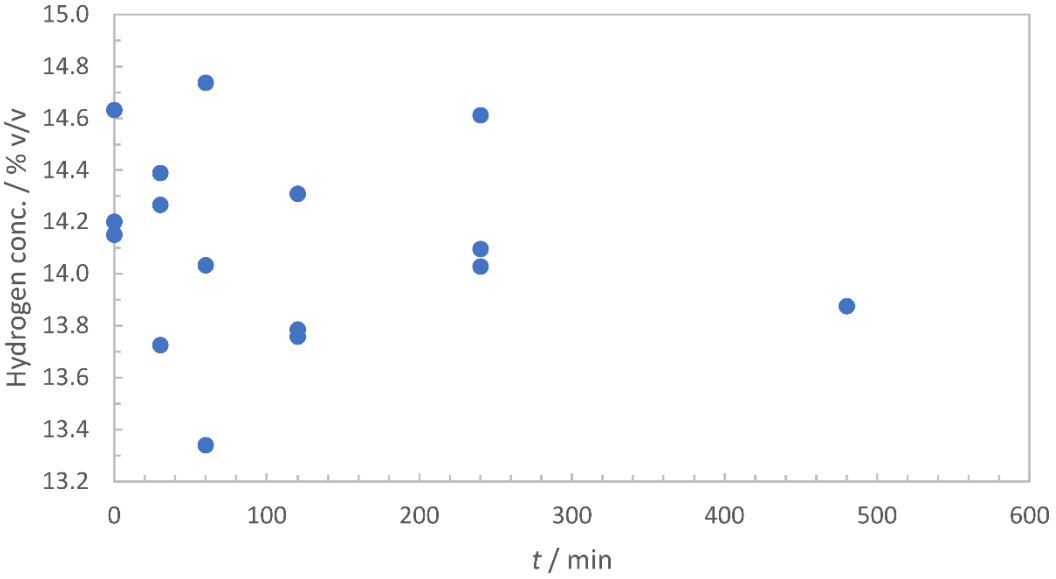

Figure 3: Measured hydrogen concentration of catalytic HER samples in dependence of the storing time.

Screening of 49 samples using the $Ru(bpy)_3(PF_6)_2$, ascorbic acid and Mo_3S_{13} HER system

For a general screening of 49 samples, catalytic samples were prepared using the procedure described above with a sample volume of 1.5 mL per vial.

Catalytic conditions: [catalyst] = 0.4 µM; [photosensitizer] = 26.6 µM; [Ascorbic Acid] = 133 mM; Solvent = organic solvent/H_2O 90:10 % v:v

Sample Preparation for Solvent Ratio and Photosensitizer Concentration Screening

Sample preparation for screening the influence of MeOH/H_2O ratio and PS concentration with 25 samples was carried out using the prepared stock solutions and the scheme depicted below.

Table 2: Volumes of stock solutions used to prepare the samples for screening of the Ru(bpy)3 sensitized HER using Mo3S13 as catalyst.

MeOH/H_2O % v/v	PS (0 µM)		PS (10 µM)		PS (20 µM)		PS (40 µM)		PS (80 µM)	
25:75	PS	0 µL	PS	12.2 µL	PS	34.4 µL	PS	68.8 µL	PS	137.6 µL
	Cat	18.6 µL	Cat	18.6 µL	Cat	18.6 µL	Cat	18.6 µL	Cat	18.6 µL
	MeOH	481.4 µL	MeOH	469.2 µL	MeOH	447 µL	MeOH	412.6 µL	MeOH	343.8 µL
	AA2	0 µL	AA2	0 µL	AA2	0 µL	AA2	0 µL	AA2	0 µL
	AA1	200 µL	AA1	200 µL	AA1	200 µL	AA1	200 µL	AA1	200 µL
	H_2O	1300 µL	H_2O	1300 µL	H_2O	1300 µL	H_2O	1300 µL	H_2O	1300 µL
50:50	PS	0 µL	PS	12.2 µL	PS	34.4 µL	PS	68.8 µL	PS	137.6 µL
	Cat	18.6 µL	Cat	18.6 µL	Cat	18.6 µL	Cat	18.6 µL	Cat	18.6 µL
	MeOH	981.4 µL	MeOH	969.2 µL	MeOH	947 µL	MeOH	912.6 µL	MeOH	843.8 µL
	AA2	0 µL	AA2	0 µL	AA2	0 µL	AA2	0 µL	AA2	0 µL
	AA1	200 µL	AA1	200 µL	AA1	200 µL	AA1	200 µL	AA1	200 µL
	H_2O	800µL	H_2O	800µL	H_2O	800µL	H_2O	800µL	H_2O	800µL
75:25	PS	0 µL	PS	12.2 µL	PS	34.4 µL	PS	68.8 µL	PS	137.6 µL
	Cat	18.6 µL	Cat	18.6 µL	Cat	18.6 µL	Cat	18.6 µL	Cat	18.6 µL
	MeOH	1481.4 µL	MeOH	1469.2 µL	MeOH	1447 µL	MeOH	1412.6 µL	MeOH	1343.8 µL
	AA2	0 µL	AA2	0 µL	AA2	0 µL	AA2	0 µL	AA2	0 µL
	AA1	200 µL	AA1	200 µL	AA1	200 µL	AA1	200 µL	AA1	200 µL
	H_2O	300 µL	H_2O	300 µL	H_2O	300 µL	H_2O	300 µL	H_2O	300 µL
90:10	PS	0 µL	PS	12.2 µL	PS	34.4 µL	PS	68.8 µL	PS	137.6 µL
	Cat	18.6 µL	Cat	18.6 µL	Cat	18.6 µL	Cat	18.6 µL	Cat	18.6 µL
	MeOH	1781.4 µL	MeOH	1769.2 µL	MeOH	1747 µL	MeOH	1712.6 µL	MeOH	1643.8 µL
	AA2	0 µL	AA2	0 µL	AA2	0 µL	AA2	0 µL	AA2	0 µL
	AA1	200 µL	AA1	200 µL	AA1	200 µL	AA1	200 µL	AA1	200 µL
	H_2O	0 µL	H_2O	0 µL	H_2O	0 µL	H_2O	0 µL	H_2O	0 µL
95:5	PS	0 µL	PS	12.2 µL	PS	34.4 µL	PS	68.8 µL	PS	137.6 µL
	Cat	18.6 µL	Cat	18.6 µL	Cat	18.6 µL	Cat	18.6 µL	Cat	18.6 µL
	MeOH	1881.4 µL	MeOH	1869.2 µL	MeOH	1847 µL	MeOH	1812.6 µL	MeOH	1743.8 µL
	AA2	100 µL	AA2	100 µL	AA2	100 µL	AA2	100 µL	AA2	100 µL
	AA1	0 µL	AA1	0 µL	AA1	0 µL	AA1	0 µL	AA1	0 µL
	H_2O	0 µL	H_2O	0 µL	H_2O	0 µL	H_2O	0 µL	H_2O	0 µL

Ordered sample placement:

Table 3: Composition of the Ru(bpy)3, Mo_3S_{13}, AA HER system and ordered sample arrangement on the 5x5 matrix of the reactor bed. See Figure 4 for detailed information on the sample position.

MeOH/H_2O % v/v	PS (0 μM)	PS (10 μM)	PS (20 μM)	PS (40 μM)	PS (80 μM)	
25:75	S21	S22	S23	S24	S25	0
50:50	S16	S17	S18	S19	S20	1
75:25	S11	S12	S13	S14	S15	2
90:10	S6	S7	S8	S9	S10	3
95:5	S1	S2	S3	S4	S5	4
	0	1	2	3	4	x/y-position

Statistical sample placement:

*Table 4: Statistical sample arrangement of the $Ru(bpy)_3$, Mo_3S_{13}, AA HER system (same chemical composition of samples as depicted in **Fehler! Verweisquelle konnte nicht gefunden werden.**) on the 5x5 matrix of the reactor bed. See Figure 4 for detailed information on the sample position.*

x/y-position	0	1	2	3	4
0	S8	S6	S19	S13	S1
1	S12	S22	S7	S20	S3
2	S14	S9	S15	S2	S24
3	S17	S16	S10	S25	S5
4	S4	S23	S18	S11	S21

Catalytic conditions: [catalyst] = 0.3 µM; [photosensitizer] = 0 µM, 10 µM, 20 µM, 40 µM, 80 µM; [Ascorbic Acid] = 100 mM ; Solvent = MeOH/H2O 25:75 % v:v, 50:50 % v:v, 75:25 % v:v, 90:10 % v:v, 95:5 % v:v

Table 5: Calculated TONs for the screened $Ru(bpy)_3$, Mo_3S_{13}, AA HER system with ordered sample arrangement.

$MeOH/H_2O$ % v/v	PS (0 µM)	PS (10 µM)	PS (20 µM)	PS (40 µM)	PS (80 µM)
25:75	0.00	42.55	234.05	489.38	1017.06
50:50	0.00	614.91	1761.76	2589.45	3636.29
75:25	0.00	1819.21	4170.35	6144.89	7238.54
90:10	0.00	2325.61	5753.38	7925.80	10989.73
95:5	0.00	1631.97	5610.83	8164.10	11153.56

Table 6: Calculated TONs for the screened Ru(bpy)3, Mo3S13, AA HER system with statistical sample arrangement.

MeOH/H_2O % v/v	PS (0 µM)	PS (10 µM)	PS (20 µM)	PS (40 µM)	PS (80 µM)
25:75	0.00	0.00	312.78	680.87	1372.39
50:50	0.00	680.87	1997.94	3519.27	5957.65
75:25	0.00	1700.06	3802.25	6059.78	9376.91
90:10	0.00	2519.23	4853.35	8674.76	10685.46
95:5	0.00	2793.71	6300.21	8093.89	10717.38

Bimane Sensitized Hydrogen Evolution

Synthesis of bimane compounds

Synthesis of 3,4-dimethyl-1H-pyrazol-5(4H)-one

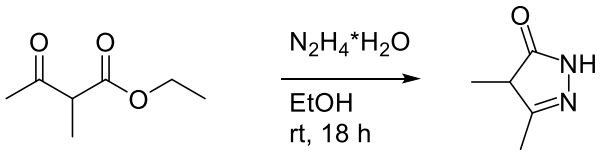

10 g (0.069 mol, 1 eq) of ethyl 2-Methyl-3-oxobutanoate was dissolved in 100 mL of EtOH in a 500 mL flask. 4.39 g of hydrazine hydrate (79% hydrazine hydrate content, 1 eq) were added to the solution and stirred at room temperature. White precipitate started to develop in the flask after about five minutes. The reaction was stirred overnight at RT, and the precipitate was filtered, washed with ethanol, and dried to yield 3.75 g (48%) of product, which was utilized without further purification.

Synthesis of *syn*-(Me,Me)Bimane

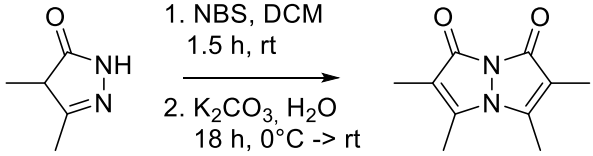

syn-(Me,Me)Bimane

Synthesis was performed with modifications of literature procedure.[3]

In a 500 mL flask 3.75 g (0.033 mol, 1 eq) of 3,4-dimethyl-1H-pyrazol-5(4H)-one was suspended in 100 mL of DCM. To this solution 5.96 g of N-Bromo-succinimide (0.033 mol, 1 eq) dissolved in 100 mL of DCM was added slowly. The resulting solution was stirred for 1 hour at RT during which the suspension became a clear pale yellow solution. The solution was cooled to 0°C, then 4.62 g K_2CO_3 (0.033 mol, 1 eq) and 0.6 mL H_2O (0.033 mol, 1 eq) were added as well. After the addition of water, suddenly very intense gas formation was observed. The flask was stirred overnight, then solvent was removed under vacuum, and the remaining solids were suspended in acetonitrile, filtered and washed with cold acetonitrile to obtain 2.6 g (78%) of pure *syn*-(Me,Me)Bimane as product.

^{1}H NMR (250 MHz, Chloroform-*d*) δ 2.29 (s, 6H), 1.80 (s, 6H).

^{13}C NMR (63 MHz, Chloroform-*d*) δ 160.94, 146.02, 112.62, 11.99, 6.89.

Synthesis of 3-methyl-1H-pyrazol-5(4H)-one

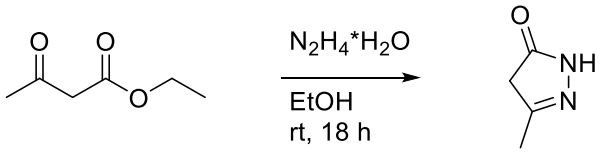

In A 500 mL flask 20 g (0.154 mol, 1 eq) of Ethyl-acetoacetate was dissolved in 250 mL of EtOH. To the solution 9.74 g of hydrazine hydrate (79% hydrazine hydrate content, 1 eq) was added and the solution was stirred at room temperature. After 5 minutes, white precipitate started to form in the flask. The reaction was stirred overnight, then the precipitate filtered, washed with ethanol, and dried to get 10.55 g (70%) of product, which was used without further purification.

Synthesis of *anti*-(Me,Br)Bimane

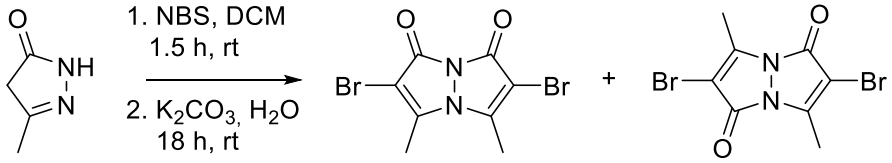

syn-(Me,Br)Bimane *anti*-(Me,Br)Bimane

Synthesis was performed with modifications of literature procedure.[3]

In a 1 L flask 10.1 g (0.107 mol, 1 eq) of 3-methyl-1H-pyrazol-5(4H)-one was suspended in 250 mL of DCM. To the solution 42 g of N-Bromo-succinimide (0.236 mol, 2.2 eq) dissolved in 250 mL of DCM was added slowly. The solution was stirred for 1.5 hours during which the suspension became a clear pale yellow solution. To this solution was then added 32.5 g K_2CO_3 (0.236 mol, 2.2 eq) and 4.2 mL H_2O (0.233 mol, 2.2 eq). After the addition of water, suddenly very intense gas formation was observed. The flask was stirred overnight at RT, then solvents were removed under vacuum, then the remaining solids were dissolved in DCM and water. The water phase was washed with DCM three times, the organic phases combined, dried with $MgSO_4$ and volatiles were removed under vacuum. The crude product (7 g) was first purified by suspending it in 50 mL acetonitrile, warming it up, sonicating, then cooling it and filtering next day, gaining 3.2 gram of yellow power containing *syn*-dibromobimane and *anti*-dibromobimane. The two products were separated using flash column chromatography (0-10% gradient elution of Ethyl-acetate in DCM) to obtain 0.91 gram (5%) of *syn*- and 1.15 gram (7%) of *anti*- and product. For photocatalytic experiments only the *anti*- form was used.

^{1}H NMR (300 MHz, Chloroform-*d*) δ 2.55 (s, 6H).

^{13}C NMR (75 MHz, Chloroform-*d*) δ 156.21, 149.49, 96.77, 12.19.

λ_{max} (1,4-dioxane): 330 nm

ε (1,4-dioxane): 14965 $M^{-1}cm^{-1}$

Sample Preparation and Photocatalysis

Sample Preparation for General Catalyst Screening

1 mM stock solutions of K_2PtCl_4, K_2PtCl_6, $PdCl_2$ + $2PPh_3$, Cobaloxime (Chloro(pyridine)cobaloxime) and Mo_3S_{13} in THF, MeOH, DMF and 1,4-Dioxane were prepared in the glovebox using 4 mL GC-vials. The stock solutions were sonicated in a water bath for 30 s, to ensure a better distribution of the used catalysts due to solubility issues. 10 mM stock solutions of dyes (*syn*- and *anti*-Bimane) in DCM were prepared. A 0.5 M solution of ascorbic acid (AA) was prepared, NH_3 (NH_3/H_2O 25 % m/m) was used to adjust the pH to 4. 200 µL of the dye stock solutions were transferred to empty 4 mL GC-vials, DCM was evaporated under Ar flow. The vials were transferred to glovebox. The samples were prepared using the pipetting scheme shown in Table 7.

Catalytic conditions: [catalyst] = 10 µM; [photosensitizer] = 1 mM; [AA] = 100 mM; solvent = organic solvent/H_2O 50/50 % v/v, 0/100 % v/v.

Table 7: Volumes of stock solutions used for sample preparation for screening the catalysts K_2PtCl_4, K_2PtCl_6, $PdCl_2$ + $2PPh_3$, Cobaloxime and Mo_3S_{13}. PS: syn-Bimane or anti-Bimane.*

50/50 % v/v	K_2PtCl_4		K_2PtCl_6		$PdCl_2$ + $2PPh_3$		Cobaloxime		Mo_3S_{13}	
THF/H_2O	PS*	200 µL	PS*	200 µL	PS*	200 µL	PS*	200 µL	PS*	200 µL
	Cat in THF	20 µL	Cat in THF	20 µL	Cat in THF	20 µL	Cat in THF	20 µL	Cat in THF	20 µL
	THF	980 µL	THF	980 µL	THF	980 µL	THF	980 µL	THF	980 µL
	AA	400 µL	AA	400 µL	AA	400 µL	AA	400 µL	AA	400 µL
	H_2O	600 µL	H_2O	600 µL	H_2O	600 µL	H_2O	600 µL	H_2O	600 µL
MeOH/H_2O	PS*	200 µL	PS*	200 µL	PS*	200 µL	PS*	200 µL	PS*	200 µL
	Cat in MeOH	20 µL	Cat in MeOH	20 µL	Cat in MeOH	20 µL	Cat in MeOH	20 µL	Cat in MeOH	20 µL
	MeOH	980 µL	MeOH	980 µL	MeOH	980 µL	MeOH	980 µL	MeOH	980 µL
	AA	400 µL	AA	400 µL	AA	400 µL	AA	400 µL	AA	400 µL
	H_2O	600 µL	H_2O	600 µL	H_2O	600 µL	H_2O	600 µL	H_2O	600 µL
DMF/H_2O	PS*	200 µL	PS*	200 µL	PS*	200 µL	PS*	200 µL	PS*	200 µL
	Cat in DMF	20 µL	Cat in DMF	20 µL	Cat in DMF	20 µL	Cat in DMF	20 µL	Cat in DMF	20 µL
	DMF	980 µL	DMF	980 µL	DMF	980 µL	DMF	980 µL	DMF	980 µL
	AA	400 µL	AA	400 µL	AA	400 µL	AA	400 µL	AA	400 µL
	H_2O	600 µL	H_2O	600 µL	H_2O	600 µL	H_2O	600 µL	H_2O	600 µL
dioxane/H_2O	PS*	200 µL	PS*	200 µL	PS*	200 µL	PS*	200 µL	PS*	200 µL
	Cat in dioxane	20 µL	Cat in dioxane	20 µL	Cat in dioxane	20 µL	Cat in dioxane	20 µL	Cat in dioxane	20 µL
	dioxane	980 µL	dioxane	980 µL	dioxane	980 µL	dioxane	980 µL	dioxane	980 µL
	AA	400 µL	AA	400 µL	AA	400 µL	AA	400 µL	AA	400 µL
	H_2O	600 µL	H_2O	600 µL	H_2O	600 µL	H_2O	600 µL	H_2O	600 µL
H_2O	PS*	200 µL	PS*	200 µL	PS*	200 µL	PS*	200 µL	PS*	200 µL
	Cat in DMF	20 µL	Cat in DMF	20 µL	Cat in DMF	20 µL	Cat in DMF	20 µL	Cat in DMF	20 µL
	AA	400 µL	AA	400 µL	AA	400 µL	AA	400 µL	AA	400 µL
	H_2O	1580 µL	H_2O	1580 µL	H_2O	1580 µL	H_2O	1580 µL	H_2O	1580 µL

Sample Preparation for Solvent Ratio and Photosensitizer Concentration Screening

1 mM stock solution of Mo_3S_{13} in DMF was prepared in the glovebox using 4 mL GC-vials. DMF was chosen as solvent due to the superior solubility of the catalysts in comparison to other solvents. Corresponding to the pipetting scheme below, a certain volume of the PS stock solution was transferred to empty 4 mL GC-vials, DCM was evaporated under Ar flow. The vials transferred to glovebox, samples prepared using the pipetting scheme shown in Table 8.

Table 8: Volumes of stock solutions used for sample preparation for screening the anti-Bimane sensitized HER using Mo_3S_{13} as catalyst.

H_2O/organic solvent % v/v	PS (0.125 mM)		PS (0.25 mM)		PS (0.5 mM)		PS (1 mM)		PS (2 mM)	
20:80	PS	25 µL	PS	50 µL	PS	100 µL	PS	200 µL	PS	400 µL
	Cat	20 µL	Cat	20 µL	Cat	20 µL	Cat	20 µL	Cat	20 µL
	dioxane	1580 µL	dioxane	1580 µL	dioxane	1580 µL	dioxane	1580 µL	dioxane	1580 µL
	AA	400 µL	AA	400 µL	AA	400 µL	AA	400 µL	AA	400 µL
	H_20	0 µL	H_20	0 µL	H_20	0 µL	H_20	0 µL	H_20	0 µL
40:60	PS	25 µL	PS	50 µL	PS	100 µL	PS	200 µL	PS	400 µL
	Cat	20 µL	Cat	20 µL	Cat	20 µL	Cat	20 µL	Cat	20 µL
	dioxane	1180 µL	dioxane	1180 µL	dioxane	1180 µL	dioxane	1180 µL	dioxane	1180 µL
	AA	400 µL	AA	400 µL	AA	400 µL	AA	400 µL	AA	400 µL
	H_20	400 µL	H_20	400 µL	H_20	400 µL	H_20	400 µL	H_20	400 µL
60:40	PS	25 µL	PS	50 µL	PS	100 µL	PS	200 µL	PS	400 µL
	Cat	20 µL	Cat	20 µL	Cat	20 µL	Cat	20 µL	Cat	20 µL
	dioxane	780 µL	dioxane	780 µL	dioxane	780 µL	dioxane	780 µL	dioxane	780 µL
	AA	400 µL	AA	400 µL	AA	400 µL	AA	400 µL	AA	400 µL
	H_20	800 µL	H_20	800 µL	H_20	800 µL	H_20	800 µL	H_20	800 µL
80:20	PS	25 µL	PS	50 µL	PS	100 µL	PS	200 µL	PS	400 µL
	Cat	20 µL	Cat	20 µL	Cat	20 µL	Cat	20 µL	Cat	20 µL
	dioxane	380 µL	dioxane	380 µL	dioxane	380 µL	dioxane	380 µL	dioxane	380 µL
	AA	400 µL	AA	400 µL	AA	400 µL	AA	400 µL	AA	400 µL
	H_20	1200 µL	H_20	1200 µL	H_20	1200 µL	H_20	1200 µL	H_20	1200 µL
99:1	PS	25 µL	PS	50 µL	PS	100 µL	PS	200 µL	PS	400 µL
	Cat	20 µL	Cat	20 µL	Cat	20 µL	Cat	20 µL	Cat	20 µL
	dioxane	0 µL	dioxane	0 µL	dioxane	0 µL	dioxane	0 µL	dioxane	0 µL
	AA	400 µL	AA	400 µL	AA	400 µL	AA	400 µL	AA	400 µL
	H_20	1580 µL	H_20	1580 µL	H_20	1580 µL	H_20	1580 µL	H_20	1580 µL

Table 9: Composition of the anti-Bimane, Mo3S13, AA HER system and sample ordered positioning on the 5x5 matrix of the reactor bed. See Figure 4 for detailed information on the sample position.

H_2O/organic solvent % v/v	PS (0.125 mM)	PS (0.25 mM)	PS (0.5 mM)	PS (1 mM)	PS (2 mM)	
25:75	S21	S22	S23	S24	S25	0
50:50	S16	S17	S18	S19	S20	1
75:25	S11	S12	S13	S14	S15	2
90:10	S6	S7	S8	S9	S10	3
95:5	S1	S2	S3	S4	S5	4
	0	1	2	3	4	x/y-position

Table 10: Statistical positioning of the samples of the anti-Bimane, Mo3S13, AA HER system (same chemical composition of samples as depicted in Figure 10) on the 5x5 matrix of the reactor bed. See Figure 4 for detailed information on the sample position.

x/y-position	0	1	2	3	4
0	S25	S2	S23	S13	S21
1	S19	S10	S15	S16	S20
2	S24	S12	S17	S14	S5
3	S18	S11	S8	S9	S6
4	S4	S1	S3	S22	S7

Catalytic conditions: [catalyst] = 10 µM; [photosensitizer] = 0.125 mM, 0.25 mM, 0.5 mM, 1 mM, 2 mM; [AA] = 100 mM; solvent = H_2O/organic solvent 20/80 % v/v, 40/60 % v/v, 60/40 % v/v, 80/20 % v/v, 99/1 % v/v.

Table 11: Calculated TONs for the screened anti-Bimane PS with ordered sample arrangement.

dioxane/H_2O % v/v	PS (0.125 mM)	PS (0.25 mM)	PS (0.5 mM)	PS (1 mM)	PS (2 mM)
20:80	6.57	14.49	24.89	46.15	68.62
40:60	22.15	48.51	90.13	136.03	202.92
60:40	41.04	77.24	134.56	194.24	288.20
80:20	24.19	41.87	68.24	79.92	151.35
99:1	10.72	17.75	30.19	38.17	28.34

Table 12: Calculated TONs for the screened anti-Bimane PS with statistical sample arrangement.

dioxane/H_2O % v/v	PS (0.125 mM)	PS (0.25 mM)	PS (0.5 mM)	PS (1 mM)	PS (2 mM)
20:80	4.53	12.13	18.45	40.21	57.45
40:60	19.15	39.26	59.17	101.75	150.07
60:40	40.34	70.09	94.09	177.33	247.99
80:20	17.11	27.70	44.36	76.41	111.26
99:1	8.11	11.94	20.36	25.66	28.72

Photonic Characterization

Rolling Bed Coverage

With the information on the dimensions of the used 4 mL GC-vials and spacing in between the different rows of vials, depicted in Figure 4, a rolling bed (reactor surface) coverage with potentially absorbing samples (vials filled with absorbing solution) of 35.1 % was calculated.

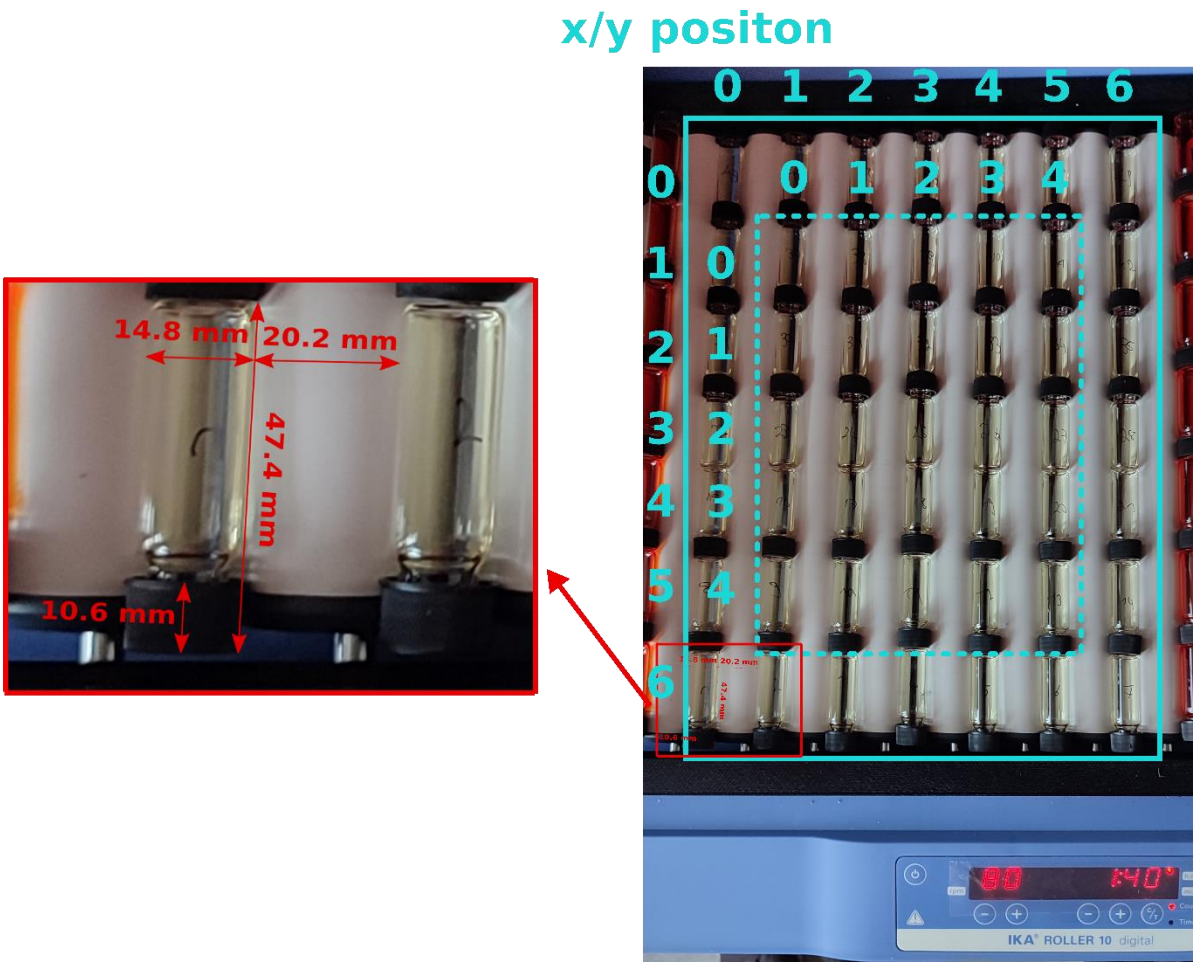

Figure 4: Vial arrangement on rolling bed (top view). With corresponding x/y positioning for the 7x7 matrix (solid line) and 5x5 matrix (dashed line). For full coverage of the reactor bed with 63 vials the most outer rows indicated with vials filled with orange solution are occupied as well.

Wavelength Dependent Emission Characteristics of LEDs

The angle dependent emission characteristics of the used 365 nm, 455 nm and 530 nm LEDs are depicted in *Figure 5*, *Figure 6* and *Figure 7*.

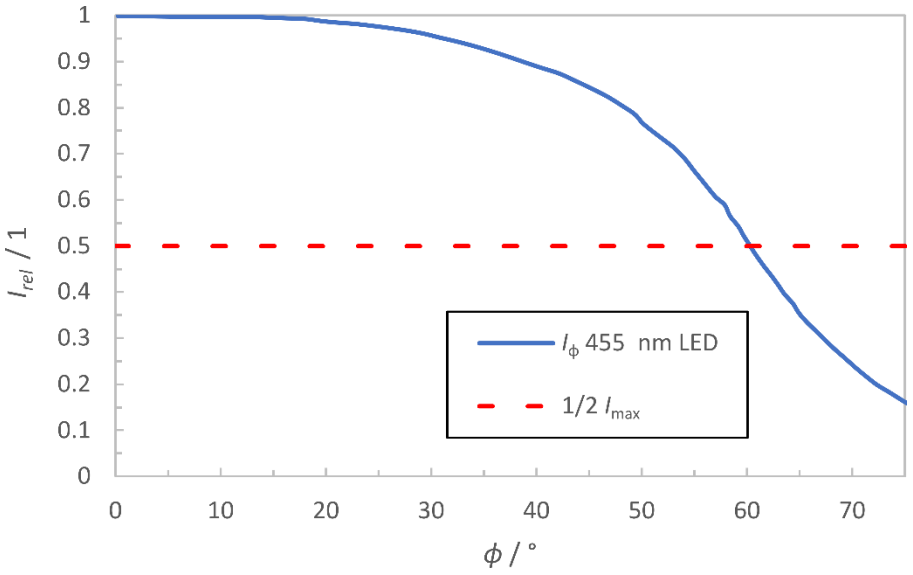

Figure 6: Emission angle dependent intensity distribution of the used 530 nm LED. [6]

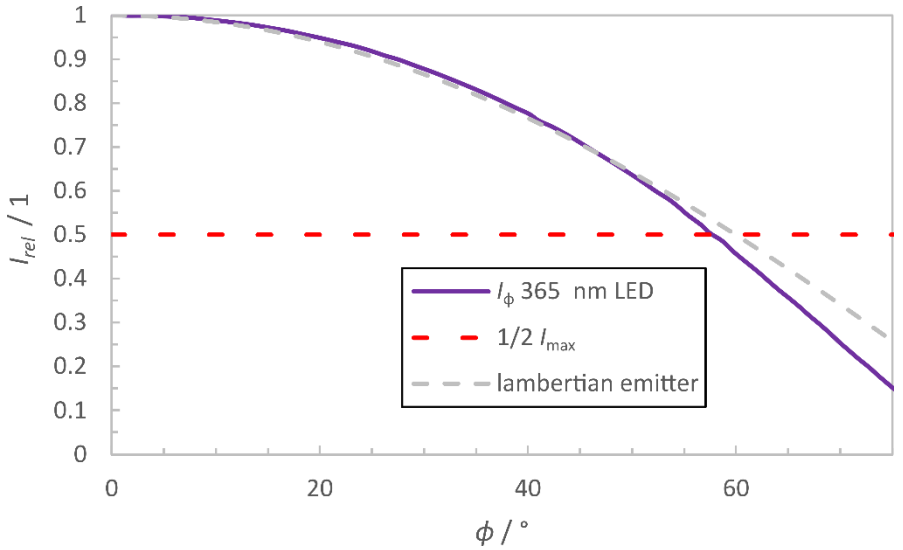

Figure 5: Emission angle dependent intensity distribution of the used 365 nm LED (solid line) in comparison to Lambertian emission (dashed line).[5]

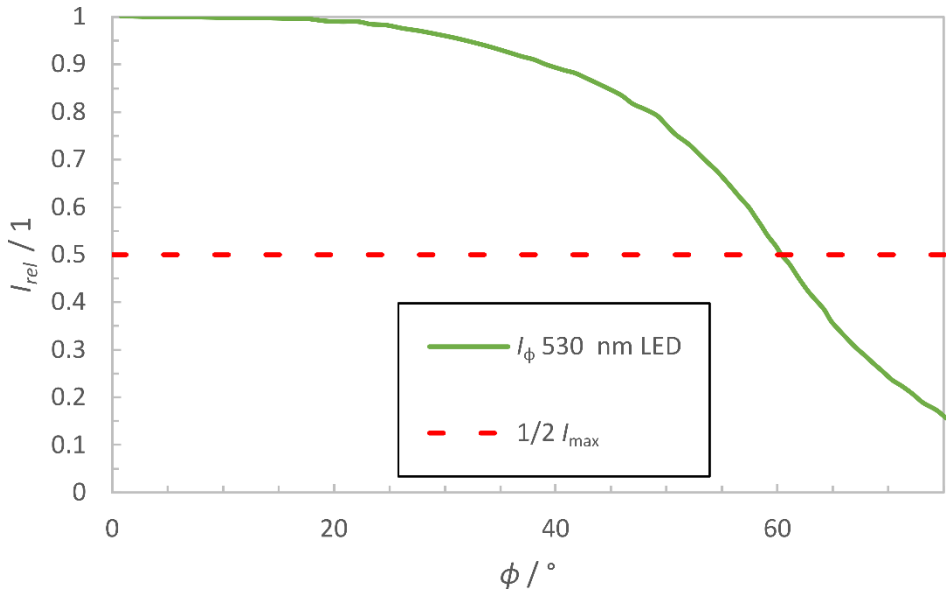

Figure 7: Emission angle dependent intensity distribution of the used 530 nm LED. [7]

Chemical Actinometry

For the actinometric experiments, the multi-batch screening photoreactor was equipped with two modules consisting of 3 LEDs each. 365 nm LEDs (LST1-0G01-UV01-00) at a constant current of 500 mA were used for all actinometric experiments. Actinometric samples of 2 mL volume were irradiated in 4 mL clear glass vials under constant mixing with an IKA Roller 10 digital at 80 rpm. After irradiation, all vials were probed immediately two times by diluting 0.5 mL of the actinometer solution with 12 mL 0.05 M H_2SO_4. All consecutive steps were performed following the modified actinometric procedure for the ferrioxalate actinometer described previously.[1] The absorbance (λ = 510 nm) of the developed solution was measured in plastic disposable UV-cuvettes (article number: 612-5503) for the UV/visible range (d = 1 cm) purchased from VWR. The actinometric procedure is based in the procedure described by Hatchard and Parker.[4]

Radiometry

Due to the emission characteristics of the used LED the distance z between the LED and the cosine corrector of the used spectrometer must be tuned to resolve the entire radiation field of the used light source. A distance of z = 10 cm equals to radius (x/y distance) of 17.3 cm in the 2D projection of the LED cone (emission angle: 60°) at the detection plane of the measurement device (see *Figure 6*), higher z distance would be bigger projections of the LED emission cone than the detection plane. Therefore, the resolution of the whole radiation field of the light source would not be possible.

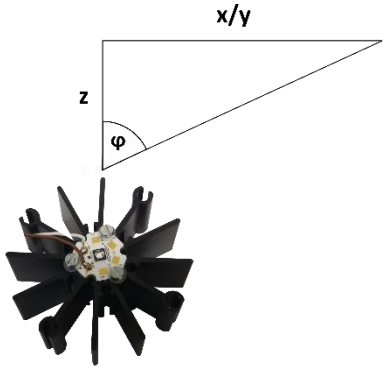

Figure 8: Depiction of the y distance dependent radius of the LEDs emission cone in x/y direction.

For all measurements, an area of 594.0 mm × 594.0 mm starting at the x/y-position (0.0 mm/0.0 mm) was scanned. For all direct measurements of the radiation sources, the LEDs were placed at a distance of 100.0 mm from the entrance of the cosine corrector of the spectrometer. This corresponded to a z-position of 35.00 mm from the x/y-plane to the z-end-stop of the radiometric box. The measured irradiation modules were placed parallel to each other at a distance of 100 mm. For all measurements applying indirect irradiation using the PTFE reflector, a z-position of 85.00 mm from the x/y-plane to the z-end-stop was used. The distance of 85.00 mm corresponded to a distance of 0.0 mm of the cosine corrector to the irradiated bed area of the multi-batch screening photoreactor. The incident radiant power of the radiation sources was calculated by calibration.

Calibration of the Radiometric Setup for the 365 nm LED (LST1-01G01-UV01-00)

The measured data of the 2D radiometry scans taken at a constant current (365 nm LED, I = 0.5 A) were corrected with a calibration factor of 0.248 to the calibration data of the supplier at the corresponding current. Comparing the raw direct with the indirect irradiation around 35.8 % of the initial direct optical power is reflected when applying the PFTE sheet.

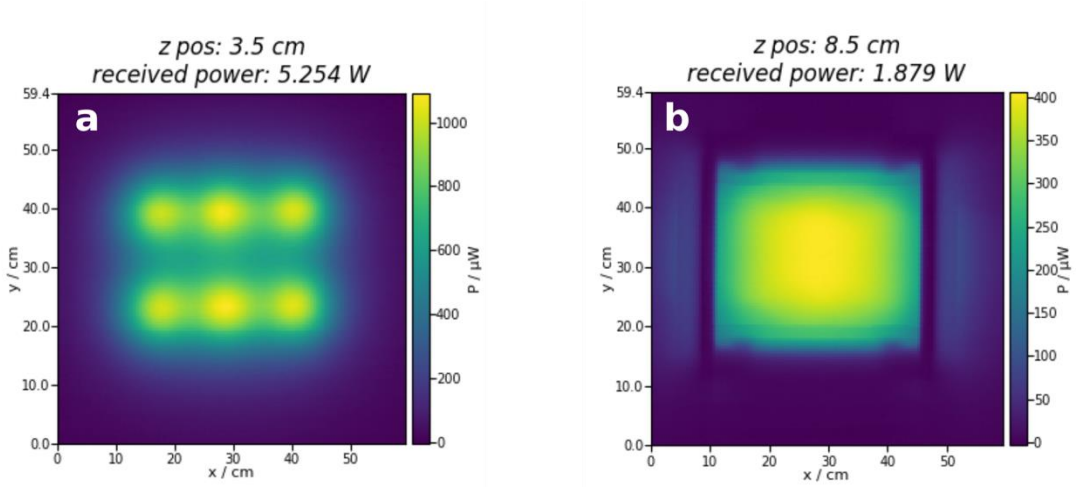

*Figure 9: Calibrated radiometric scans of direct irradiation using **a:** 6 365 nm LEDs and **b:** indirect irradiation using a PTFE reflector.*

Calibration of the Radiometric Setup for the 455 nm LED (LST1-01F06-RYL1-00)

The measured data of the 2D radiometry scans taken at a constant current (455 nm LED, *I* = 0.35 A, *I* = 0.7 A and *I* = 1.0 A) were corrected with a calibration factor of 0.287, 0.260 and 0.272 to the calibration curve derived from the optical powers of the manufacturers data sheet at 0.35 A and 0.7 A shown in Figure 10.

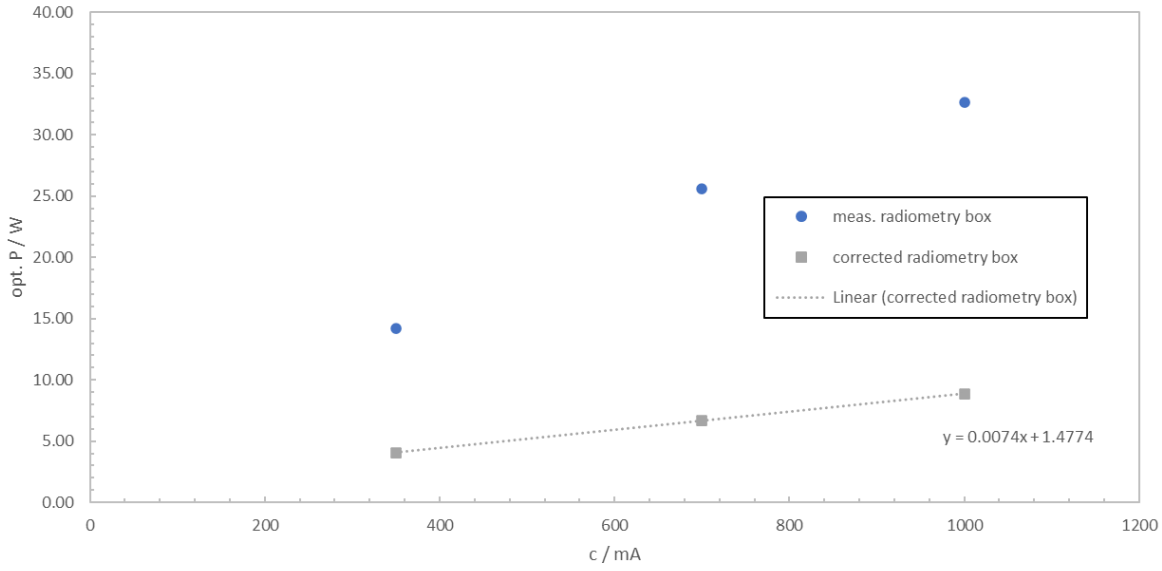

Figure 10: Measured raw and calculated corrected optical powers derived from 2D radiometric scans for the used 6 455 nm LED.

Comparing the raw direct and indirect irradiation, around 37.3 % of initial intensity left using 2 mm PTFE reflector and 455 nm LEDs at 1000 mA current.

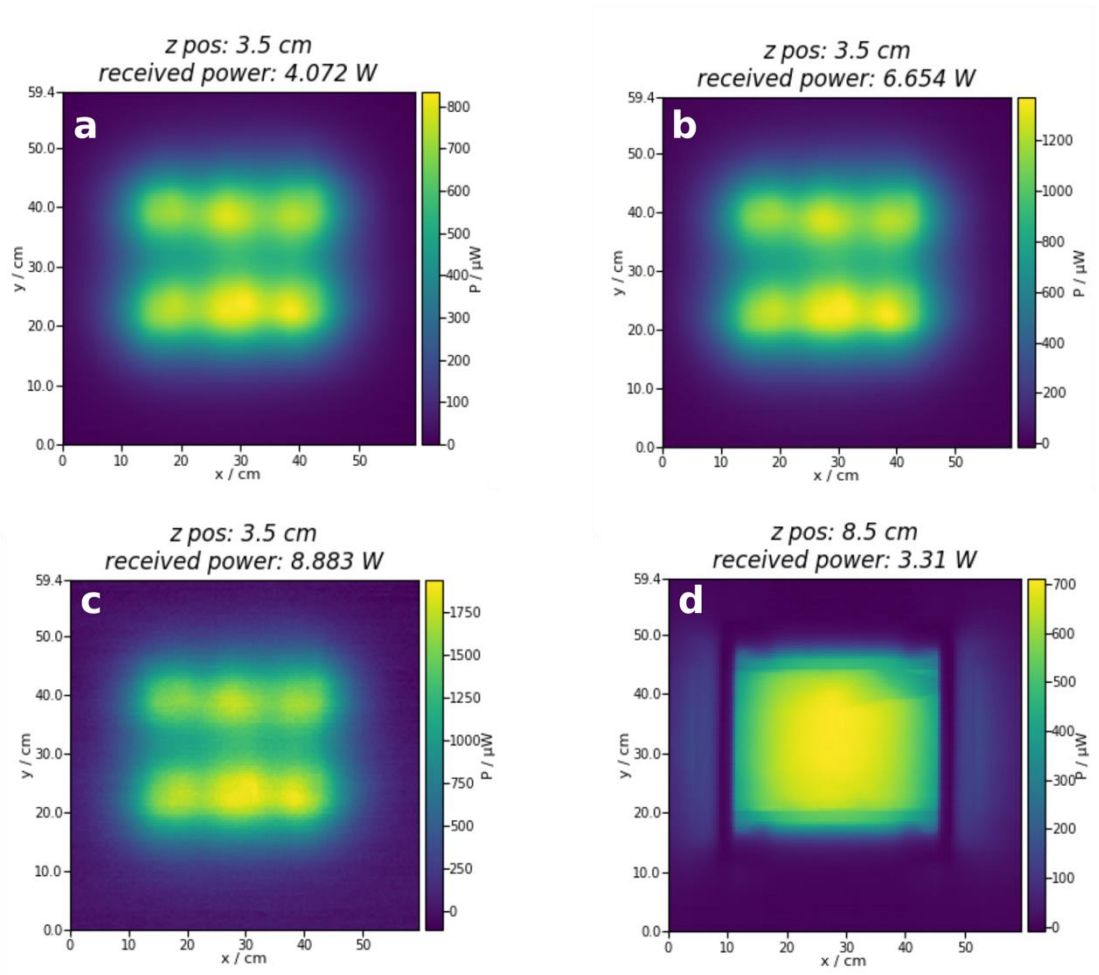

*Figure 12: Calibrated 2D radiometric measurements of the used 6 455 nm LEDs applying direct irradiation at **a:** 350 mA, **b:** 700 mA, **c:** 1000 mA and **d:** application of the PTFE reflector at 1000 mA.*

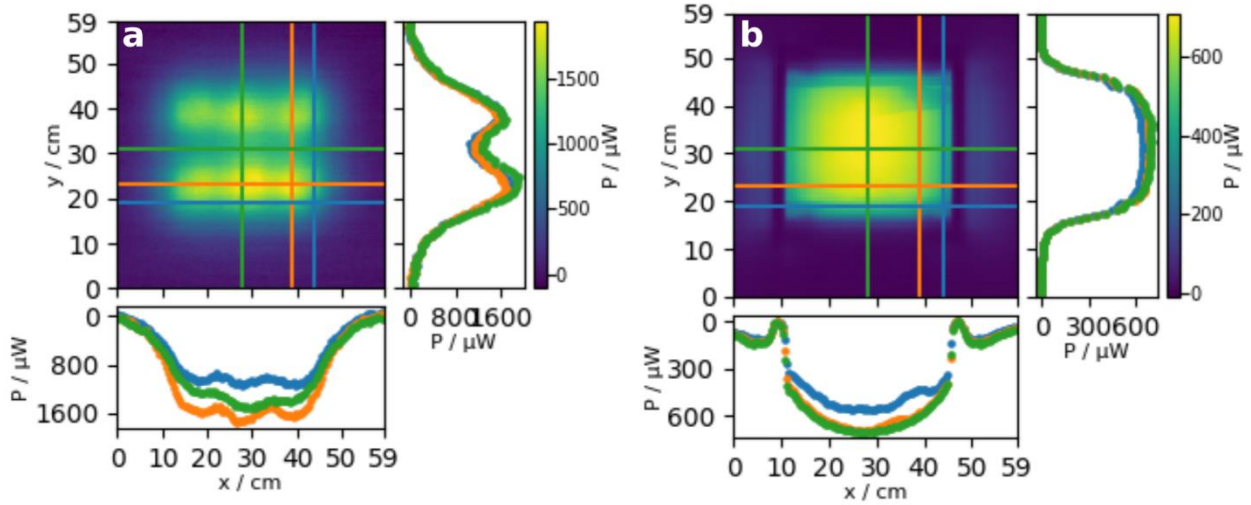

*Figure 11: Evaluation of the spatially resolved intensity distribution along x- and y-slices for **a:** direct and **b:** indirect irradiation using 6 455 nm LEDs and a PTFE reflector.*

Calibration of the Radiometric Setup for the 530 nm LED (LST1-01F06-GRN1-00)

The measured data of the 2D radiometry scans taken at a constant current (530 nm LED, *I* = 0.35 A, *I* = 0.7 A and *I* = 1.0 A) were corrected with a calibration factor of 0.313, 0.243 and 0.257 to the calibration curve derived from the optical powers of the manufacturers data sheet at 0.35 A and 0.7 A shown in Figure 13.

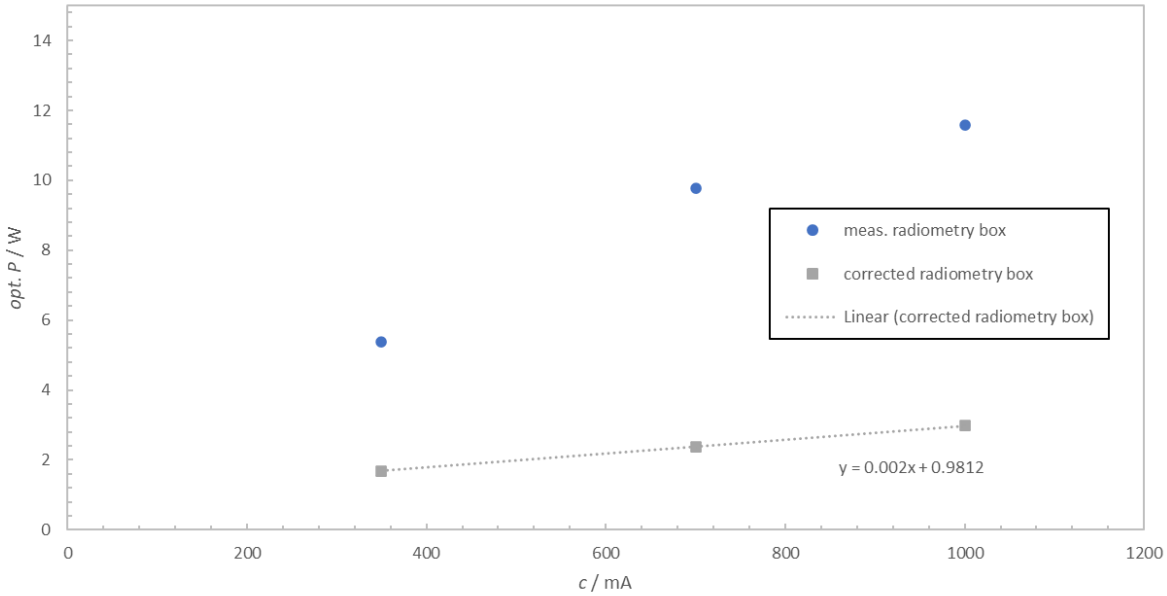

Figure 13: Measured raw and corrected calibrated optical powers derived from 2D radiometric scans for the used 6 530 nm LED.

Comparing the raw direct and indirect irradiation, around 34.7 % of initial intensity left using 2 mm PTFE reflector and 530 nm LEDs at 1000 mA current.

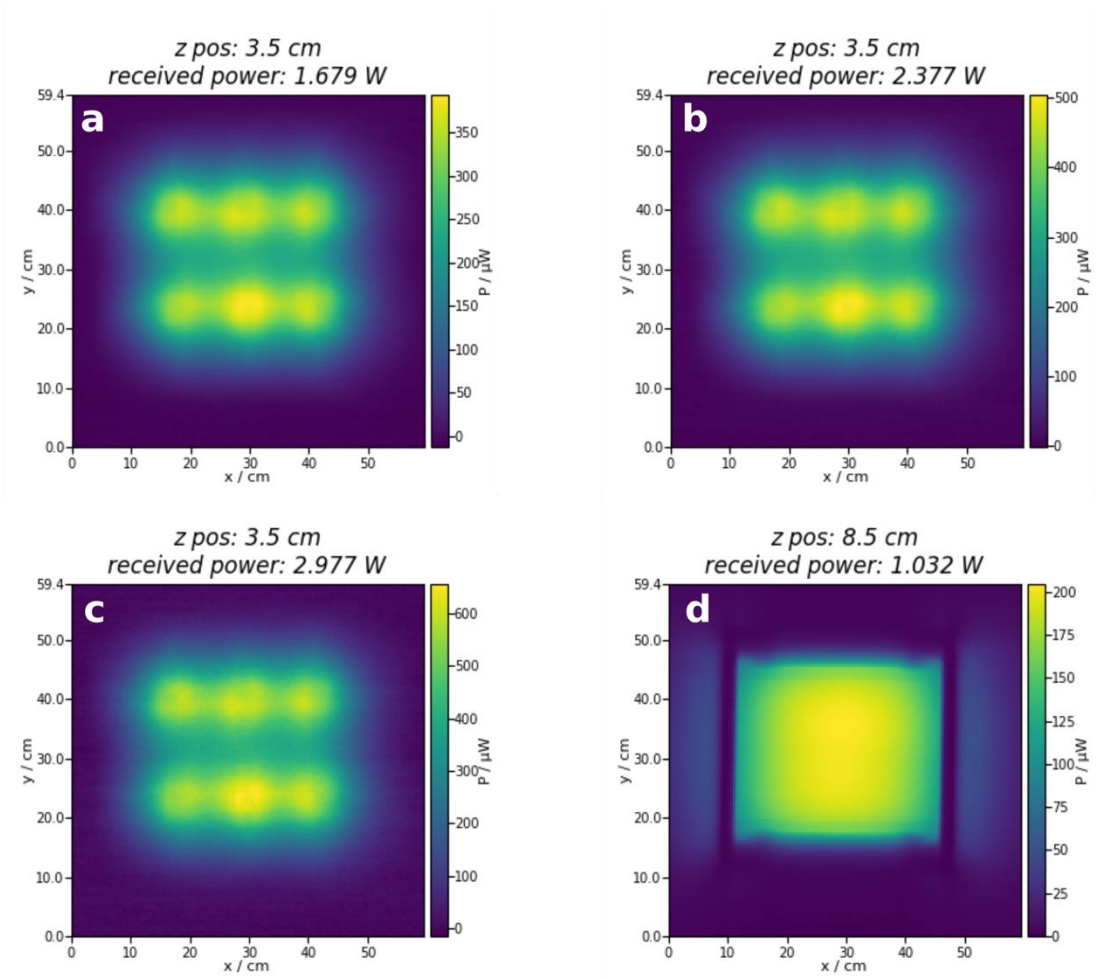

Figure 14: Calibrated 2D radiometric measurements of the used 6 530 nm LEDs applying direct irradiation at a: 350 mA, b: 700 mA, c: 1000 mA and indirect irradiation using a PTFE reflector at d: 1000 mA.

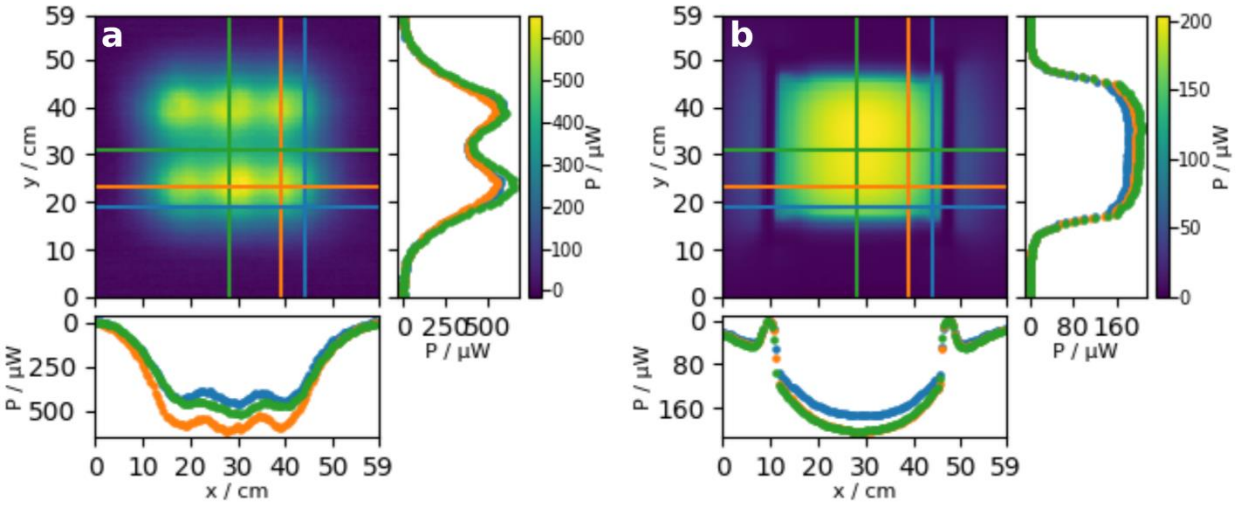

*Figure 15: Evaluation of the spatially resolved intensity distribution along x- and y-slices for **a:** direct and **b:** indirect irradiation using 6 530 nm LEDs.*

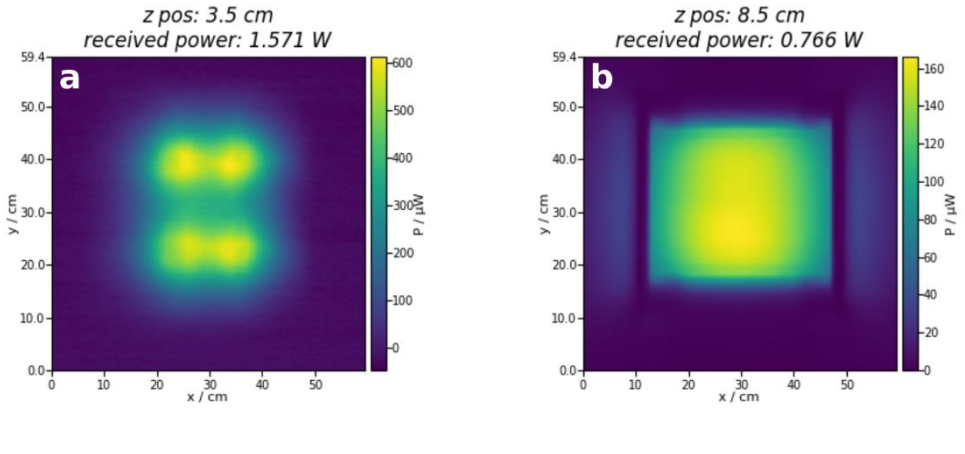

*Figure 16: Calibrated 2D radiometric measurements of the used 4 530 nm LEDs applying direct irradiation at **a:** 1000 mA, and indirect irradiation using **b:** a PTFE reflector at 1000 mA.*

Wavelength Dependent Reflective Properties of the Reactor Material

Different reflecting materials (aluminum sheet 0.08 mm, polished steel sheet 2.0 mm, virginal technical PTFE 0.1-3.0 mm and optical PTFE 2.0 mm) were tested for their reflective properties in comparison to a mirror reference Avantes RS-2. The measurements were carried out as described by Kowalczyk et al.[1] For all measurements a 50 µm slit Avantes Slit-50-RS was installed at the spectrometer. The results of the measurements are depicted in Figure 17.

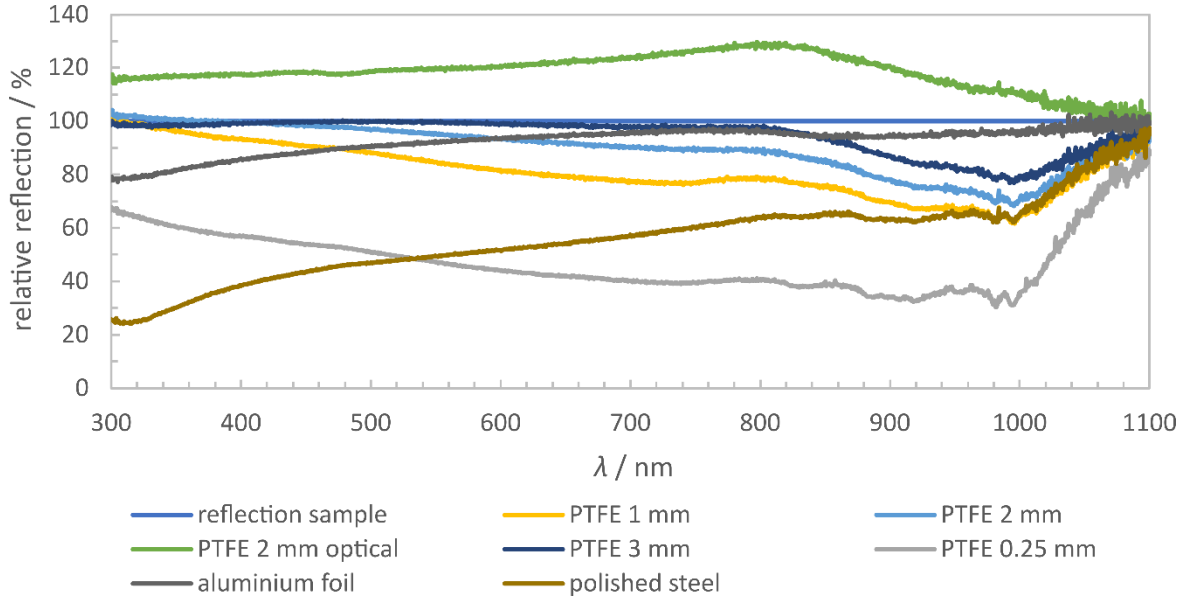

Figure 17: Wavelength dependent relative reflectance of a 0.08 mm aluminum sheet, 2.0 mm polished steel sheet, 0.25-3.0 mm virginal technical PTFE and a 2.0 mm optical PTFE sheet.

Spectroscopic data of *anti*-(Me,Br)bimane

For determining the molar absorption coefficient of *anti*-(Me,Br)bimane, the absorption spectrum in 1,4-dioxane at 80, 40, 20, 10, 5 and 2.5 µM concentrations was recorded and plotted the maximal values

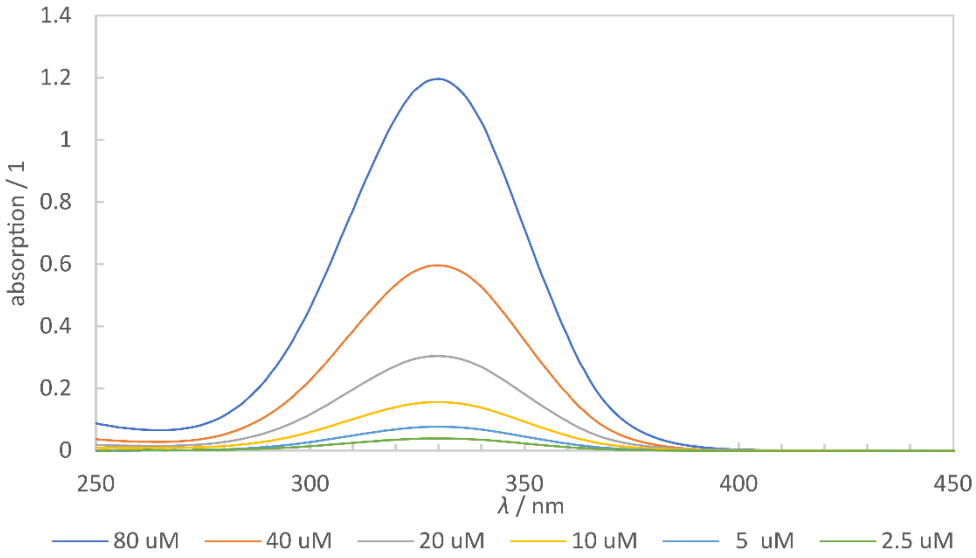

Figure 18: Concentration dependent absorption of anti-(Me,Br)Bimane in 1,4-dioxane.

obtained at 330 nm versus the concentration. The steepness of the fitted trendline gave a molar absorption coefficient of 14965 $M^{-1}cm^{-1}$.

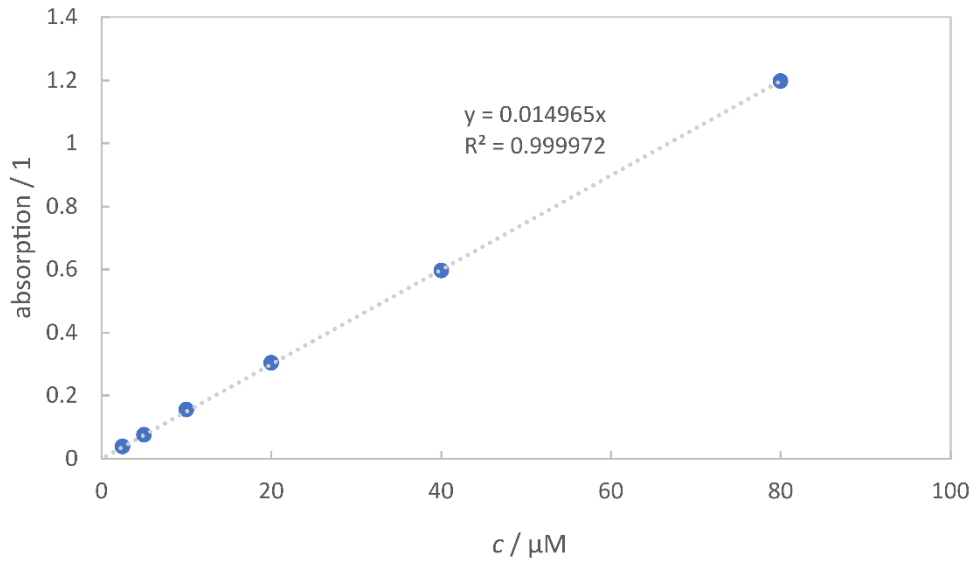

Figure 19: Absorption of anti-(Me,Br)bimane at 330 nm in 1,4-dioxane for the determination of the molar absorption coefficient.

NMR spectra of bimanes

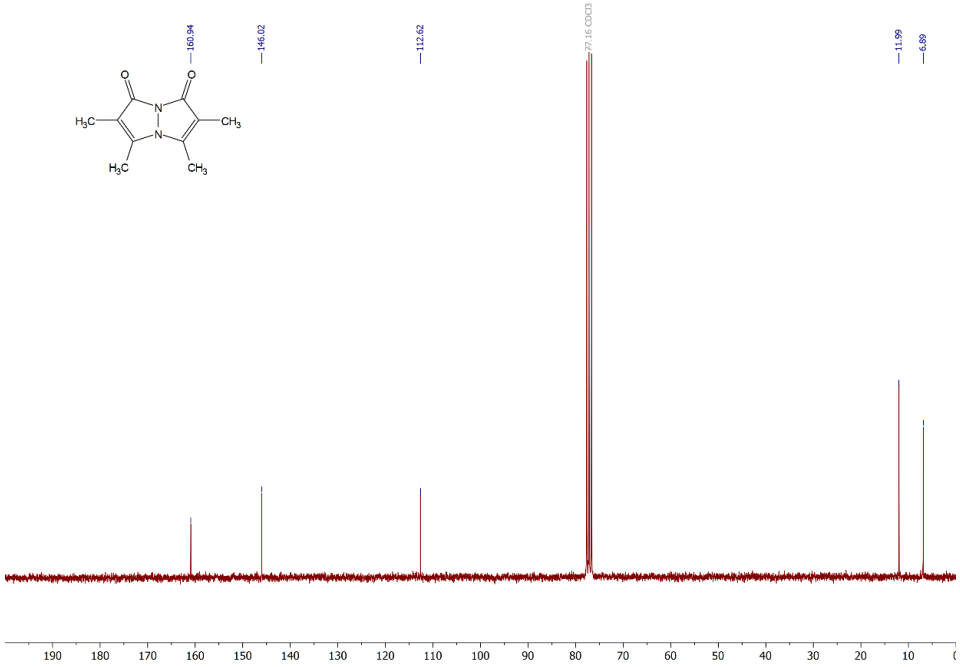

Figure 20: ^{1}H NMR of syn-(Me,Me)Bimane in $CDCl_3$.

syn-(Me,Me)Bimane

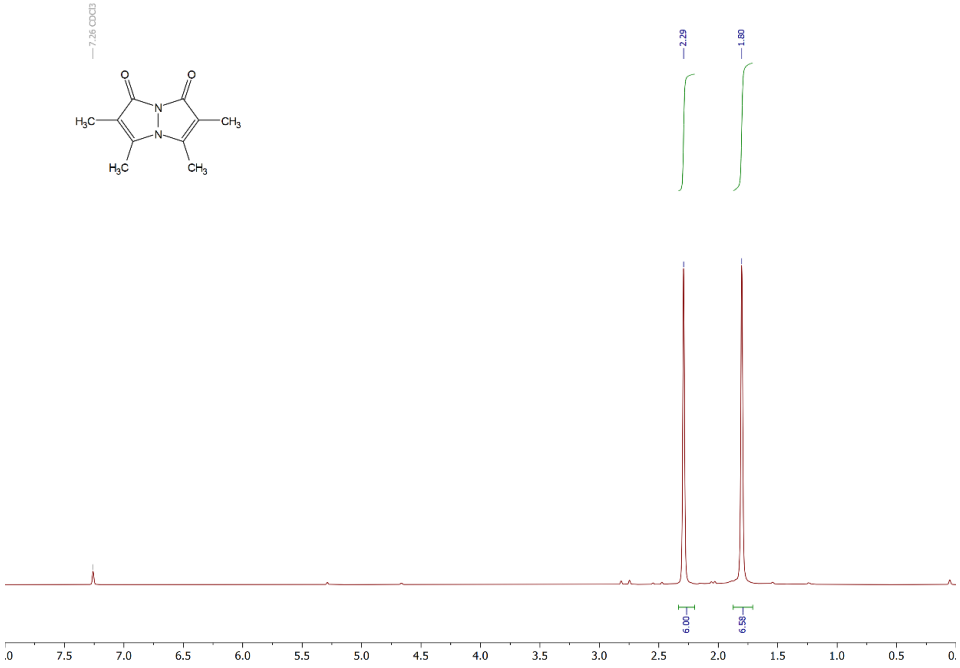

Figure 21: ^{13}C NMR of syn-(Me,Me)Bimane in $CDCl_3$.

anti-(Me,Br)Bimane

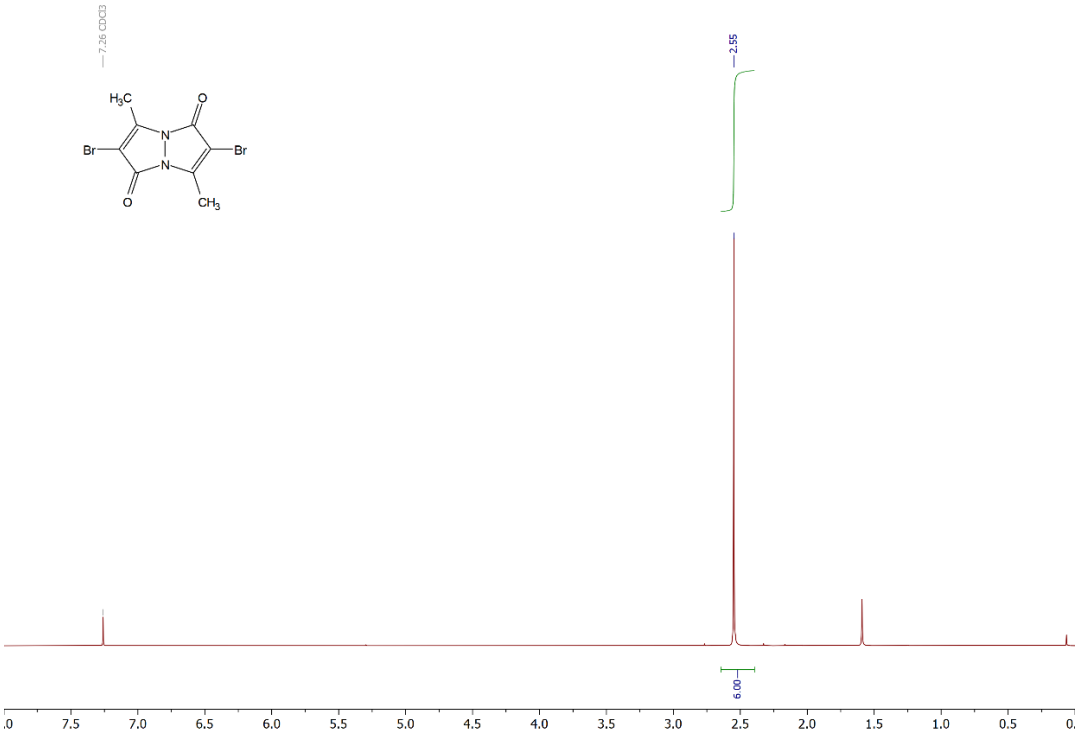

Figure 22: ^{1}H NMR of anti-(Me,Br)Bimane in $CDCl_3$.

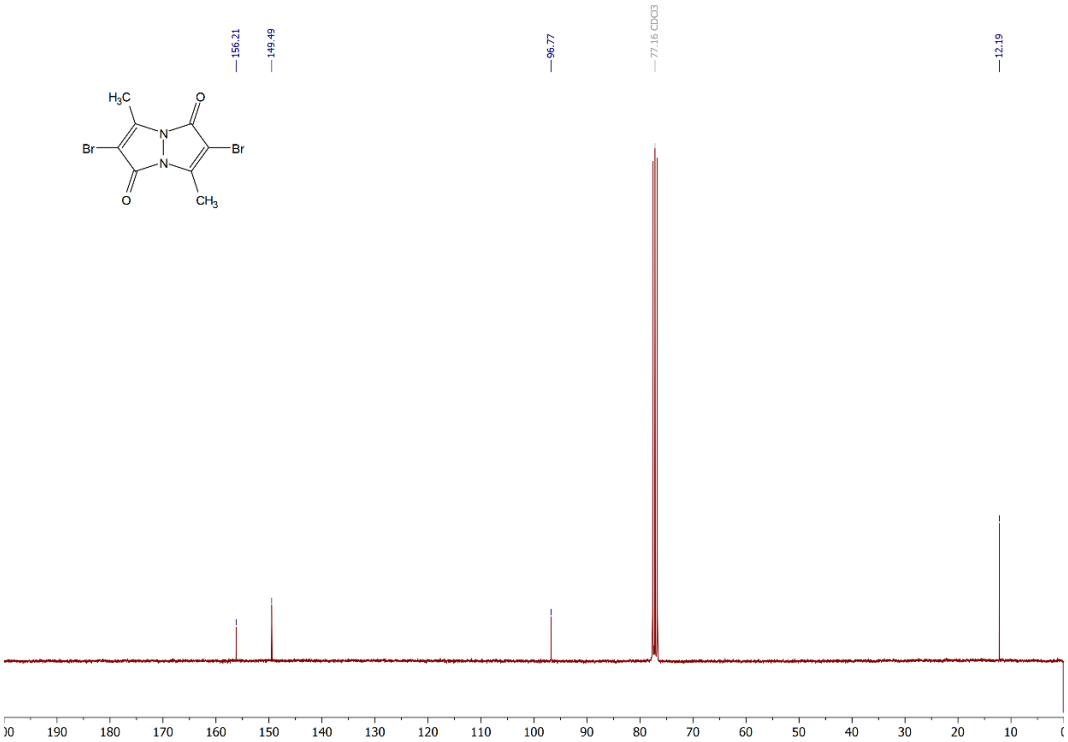

Figure 23: ^{13}C NMR of anti-(Me,Br)Bimane in $CDCl_3$.

Sources

[1] D. Kowalczyk, P. Li, A. Abbas, J. Eichhorn, P. Buday, M. Heiland, A. Pannwitz, F. H. Schacher, W. Weigand, C. Streb, D. Ziegenbalg, *ChemPhotoChem* **2022**, DOI doi.org/10.1002/cptc.202200044.

[2] A. Müller, S. Pohl, M. Dartmann, J. P. Cohen, J. M. Bennett, R. M. Kirchner, *Zeitschrift für Naturforsch. B* **1979**, *34*, 434–436.

[3] and B. P. Edward M. Kosower, *J. Am. Chem. Soc.* **1980**, *102*, 4983–4993.

[4] C. A. P. C. G. Hatchard, *Proc. R. Soc. London. Ser. A. Math. Phys. Sci.* **1956**, *235*, 518–536.

[5] *Inc., Luminus Devices SST-10-UV Product Datasheet*, **2018**.

[6] *Datasheet OSRAM OSLON® SSL 120 Deep Blue*, **2017**.

[7] *Datasheet OSRAM OSLON® SSL 120 True Green*, **2018**.